

Research Article

SENSING ABILITY OF Zn-TETRAPHENYLPORPHYRIN LANGMUIR-SCHAEFER FILMS

O. V. Maltceva<sup>1</sup>, K. S. Nikitin<sup>1</sup>, A. V. Kazak<sup>2,3</sup>, N. Zh. Mamardashvili<sup>1\*</sup>, N. V. Usol'tseva<sup>2</sup>

<sup>1</sup>G. A. Krestov Institute of Solution Chemistry of the Russian Academy of Sciences, Ivanovo, Russia

<sup>2</sup>Nanomaterials Research Institute, Ivanovo State University, Ivanovo, Russia

<sup>3</sup>Moscow Polytechnic University, Moscow, Russia

---

ARTICLE INFO:

Article history:

Received 17 April 2023

Approved 17 May 2023

Accepted 22 May 2023

---

Key words:

Langmuir-Schaefer films,  
Zn-tetraphenylporphyrin,  
sensing ability

---

ABSTRACT

The floating layers formation conditions of Zn(II)-5,10,15,20-tetraphenylporphyrin (ZnTPP) at the air/water interface and Langmuir-Schaefer films (LS-films) obtained on glass and silicon substrates have been studied. The floating layers were modeled and the geometric characteristics of molecular packings on water surface were calculated. It was shown that the area per molecule in the dense *face-on* packing of a monolayer is 1.69 nm<sup>2</sup>, and in the *edge-on* packing – 0.90 nm<sup>2</sup>. Analysis of the floating layer compression isotherm revealed that ZnTPP molecules are arranged *face-on* to the interface plane. Electron absorption spectroscopy showed that LS-films contain aggregates of J-type. The surface morphology of LS-films studied by AFM revealed that the average roughness of LS-films increases by 1.4 times with an increase in the number of transfers from one to five. The sensing properties of the LS-films (with 15 transfers) with respect to hydroxypyridine and pyridine in aqueous and gaseous media, correspondingly, have been studied. It was established that the LS-film is sensitive to pyridine vapors. The results obtained can be used to create selective sensors for environmental pollution monitoring.

---

DOI:

10.18083/LCAppl.2023.2.29

---

For citation:

Maltceva O. V., Nikitin K. S., Kazak A. V., Mamardashvili N. Zh., Usol'tseva N. V. Sensing ability of Zn-tetraphenylporphyrin Langmuir-Schaefer films. *Liq. Cryst. and their Appl.*, 2023, **23** (2), 29–37.

---

\*Corresponding author: [ngm@isc-ras.ru](mailto:ngm@isc-ras.ru)

© Maltceva O. V., Nikitin K. S., Kazak A. V., Mamardashvili N. Zh., Usol'tseva N. V., 2023

**Научная статья**

УДК 532.783:539.216

**СЕНСОРНАЯ СПОСОБНОСТЬ Zn-ТЕТРАФЕНИЛПОРФИРИНОВЫХ  
ПЛЕНОК ЛЕНГМЮРА-ШЕФФЕРА**О. В. Мальцева<sup>1</sup>, К. С. Никитин<sup>1</sup>, А. В. Казак<sup>2,3</sup>, Н. Ж. Мамардашвили<sup>1\*</sup>, Н. В. Усольцева<sup>2</sup><sup>1</sup>Институт химии растворов им. Г. А. Крестова Российской академии наук, Иваново, Россия<sup>2</sup>НИИ наноматериалов, Ивановский государственный университет, Иваново, Россия<sup>3</sup>Московский политехнический университет, Москва, Россия**ИНФОРМАЦИЯ****История статьи:**

Поступила 17.04.2023

Одобрена 17.05.2023

Принята 22.05.2023

**Ключевые слова:**

Пленки

Ленгмюра-Шеффера,

Zn-тетрафенилпорфирин,

сенсорная способность

**АННОТАЦИЯ**

Изучены условия формирования плавающих слоев Zn(II)-5,10,15,20-тетрафенилпорфирина (ZnTPP) на границе воздух/вода и пленок Ленгмюра-Шеффера (ЛШ-пленок) на стеклянных и кремниевых подложках. Смоделированы плавающие слои и рассчитаны геометрические характеристики молекулярных упаковок на поверхности воды. Показано, что площадь, приходящаяся на одну молекулу, в плотной упаковке монослоя *face-on* составляет 1,69 нм<sup>2</sup>, а *edge-on* – 0,90 нм<sup>2</sup>. Анализ изотермы сжатия плавающего слоя показал, что молекулы ZnTPP располагаются *face-on* геометрии на поверхности субфазы. При помощи электронных спектров поглощения установлено, что исследуемые наноматериалы содержат агрегаты J-типа. Морфология поверхности ЛШ-пленок, изученная методом АСМ, показала, что средняя шероховатость ЛШ-пленок увеличивается в 1,4 раза при увеличении числа переносов от одного до пяти. Исследованы чувствительность и связывающие свойства ЛШ-пленок (с 15 переносами) по отношению к гидроксипиридину и пиридину в водной и газовой средах соответственно. Установлено, что ЛШ-пленка чувствительна к парам пиридина. Полученные результаты могут быть использованы для создания селективных сенсоров для мониторинга загрязнения окружающей среды.

**DOI:**

10.18083/LCAppl.2023.2.29

**Для цитирования:**

Мальцева О. В., Никитин К. С., Казак А. В., Мамардашвили Н. Ж., Усольцева Н. В. Сенсорная способность Zn-тетрафенилпорфириновых пленок Ленгмюра-Шеффера // Жидк. крист. и их практич. использ. 2023. Т. 23, № 2. С. 29–37.

\*Адрес для переписки: ngm@isc-ras.ru

© Мальцева О. В., Никитин К. С., Казак А. В., Мамардашвили Н. Ж., Усольцева Н. В., 2023

## Introduction

Our research over the past decade has been focused on the systematic development of new porphyrins of complex structure that exhibit sensing and binding properties in solutions [1–4]. At the same time, the analysis of literature data and our own research results show that along with sensing properties porphyrins may have a high ability to supramolecular self-assembly [1–5]. Molecular self-assembly is the formation process of a complex ordered supramolecular structure, in which the structure of "assembling" molecules remains almost unchanged [6–10]. The presence of functional groups of a certain nature makes it possible to obtain 2D and 3D structures with specified dimensions and properties [11–14]. In the works [15–21], authors give examples of such self-assembled structures obtained by Langmuir methods. Self-assembly of porphyrins can occur both in solutions [22] and in floating layers [22–23]. The self-assembly process can be used to obtain functional nanomaterials with a wide range of practical applications. It should be noted that the physical and chemical properties of porphyrins thin films differ significantly from the properties of individual molecules in solution [19] and, as a consequence, the sensing and binding properties will be different.

The presented work is devoted to determining conditions for the formation and characterization of LS-films based on ZnTPP as well as evaluating sensing and binding properties of film samples to 3-hydroxypyridine (PyOH) and pyridine (Py) in aqueous and gaseous media, respectively.

## Experimental

### Materials

*Zn(II)-5,10,15,20-tetraphenylporphyrin*. 0.05 g (0.0813 mmol) of tetraphenylporphyrin and 0.144 g (0.813 mmol) of  $\text{Zn}(\text{OAc})_2$  were dissolved in DMF (70 ml), and the mixture was refluxed for 1 hour and then cooled. The filtrate was poured into water and the formed precipitate was filtered, washed with water, dried and chromatographed on aluminum oxide using dichloromethane as an eluent. Yield 0.04 g (0.058 mmol, 72 %),  $R_f$  0.78 (hexane–chloroform, 1:1). IR spectrum,  $\nu$ ,  $\text{cm}^{-1}$ : 2917, 2849 (CH, Ph), 1694, 1599 (C=C, Ph),

1437 (C=N), 1350 (C–N), 1150, 1073 [ $\delta$ (C–H, Ph)], 1004 (Co–N), 796 [ $\gamma$ (C–H, pyrrole ring)], 752, 702 [ $\gamma$ (C–H, Ph)], 470 (Zn–N). NMR  $^1\text{H}$  spectrum ( $\text{CDCl}_3$ ),  $\delta$ , m. d.: 9.05 d (8H, pyrrole), 7.67 d (8H,  $\text{Ph}_{\text{ortho}}$ ), 7.59 t (8H,  $\text{Ph}_{\text{meta}}$ ,  $J$  7.7 Hz), 7.33 t (4H,  $\text{Ph}_{\text{para}}$ ). Mass spectrum,  $m/z$  (I rel, %): 677.1 (99) [ $\text{M}-\text{H}$ ] $^+$  (calculated for  $\text{C}_{44}\text{H}_{28}\text{N}_4\text{Zn}$ : 678.1). UV-vis spectrum (benzene),  $\lambda_{\text{max}}$ , nm (lg $\epsilon$ ): 584 (4.16), 547 (3.65), 418 (5.35). Found, %: C 78.68; H 4.17; N 8.30.  $\text{C}_{44}\text{H}_{28}\text{N}_4\text{Zn}$ . Calculated, %: C 78.71; H 4.20; N 8.33.

5,10,15,20-tetraphenylporphyrin (99.9 %), pyridine (Py, 99.7 %), 3-hydroxypyridine (PyOH, 99.4 %) and chloroform (>99.8 %) of Sigma-Aldrich (France) were used without additional purification.

### Methods

Electronic absorption spectra of thin films were obtained using a Cary 300 spectrophotometer at 295 K.  $^1\text{H}$  NMR spectra were registered using a Bruker AVANCE-500 instrument (internal standard – TMS). Mass spectra were recorded on a Shimadzu Biotech Amino Confidence Maldi TOF mass spectrometer (matrix – dihydroxybenzoic acid). IR spectra were recorded on an infrared VERTEX 80v Fourier spectrometer. Elemental analysis was performed on a CHN FlashEA 1112 analyzer. Surface microrelief of LS-films was studied on a scanning probe device of atomic force microscopy (AFM) Solver 47-PRO in semi-contact mode.

Taking into account the experimental data of [23], which showed that Ni(II)-5,10,15,20-tetraphenylporphyrin is capable of taking both *face-on* and *edge-on* orientation at the air/water interface, we conducted the simulation of ZnTPP floating layer according to these two orientation scenarios. After optimization by the molecular mechanics method in the HyperChem 8.1 program, the *face-on* and *edge-on* models of a monomolecular floating layer at the air/water interface were obtained (Fig. 1). Based on these calculations, the areas of the dense ZnTPP packings were estimated. The area per molecule in the dense *face-on* packing ( $A_{\text{pack}(\text{face})}$ ) was found equal to 1.69  $\text{nm}^2$ , and in the case of *edge-on* packing ( $A_{\text{pack}(\text{edge})}$ ) – 0.90  $\text{nm}^2$  (Fig. 1). These values were compared with the area at the transfer point of the floating layer compression isotherm. On the basis of these results, a conclusion was drawn about the structure of the floating layer.

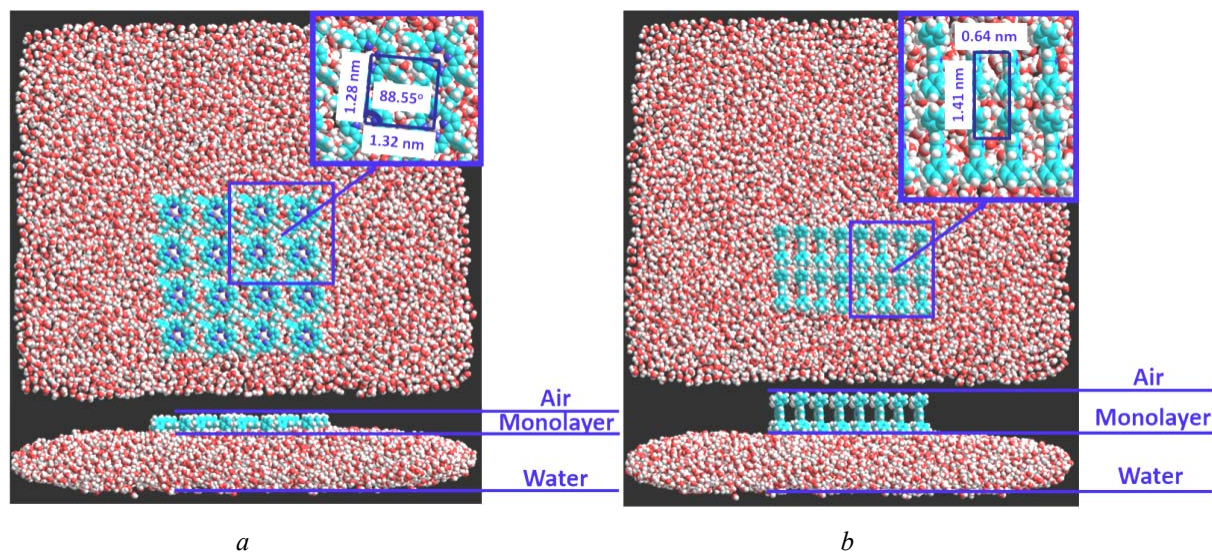


Fig. 1. The models of *face-on* (a) and *edge-on* (b) monolayer packings of ZnTPP molecules on the air/water interface

The geometric parameters of the ZnTPP molecule were calculated using the molecular model shown in Fig. 2. The projection areas for the molecule in *face-on* and *edge-on* orientations were  $1.43 \text{ nm}^2$  and  $0.71 \text{ nm}^2$ , correspondingly.

Floating layers were obtained from chloroform solution ( $C = 1.5 \cdot 10^{-4} \text{ M}$ ) using NT-MDT Langmuir trough (Zelenograd, Russia). To obtain floating layers, the solution was applied to the surface of bidistilled water at  $295 \pm 1 \text{ K}$ . 30 minutes after applying the

solution, the floating layer was compressed at a rate of  $55 \text{ cm}^2/\text{min}$ . When applying the solution, the initial degree of water surface coverage with ZnTPP was  $c_{\text{face}} = 69 \%$ . It was calculated according to the method described in [24]. With a 100 % degree of surface coating, the barriers in the bath were stopped and the floating layer was sequentially transferred to glass or silicon substrates by the Langmuir-Schaefer method according the procedure described in [24].

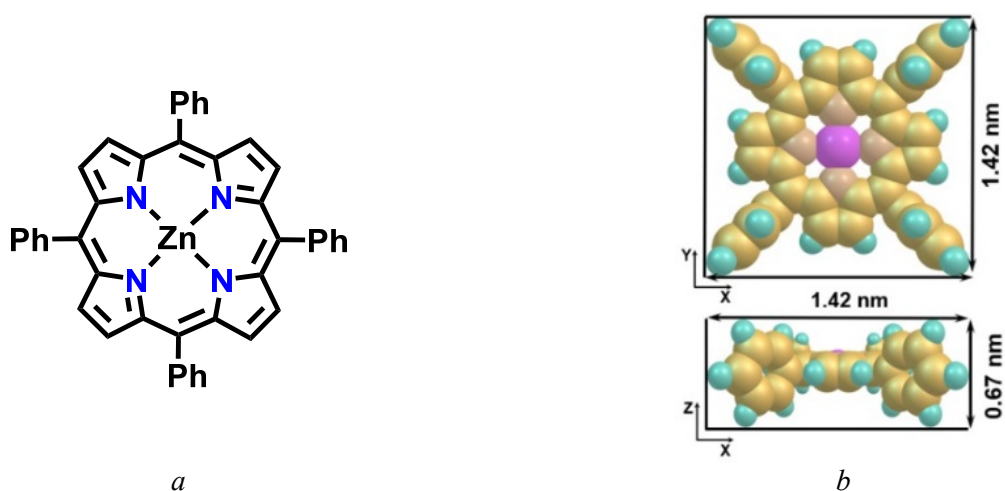


Fig. 2. Chemical structure (a) and geometric model (b) of ZnTPP



## Results and discussions

### Morphology of ZnTPP LS-films

To study the surface morphology of the ZnTPP LS-films, the floating layer was transferred with varying numbers of transfers onto silica substrate. The transfers were carried out when the area per molecule in the floating layer was  $1.52 \text{ nm}^2$ . Comparison of this value with the calculated values of  $A_{\text{pack}(\text{face})}$  and  $A_{\text{pack}(\text{edge})}$  allows us to conclude that at the transfer point (Fig. 3) ZnTPP molecules are in the *face-on* orientation.

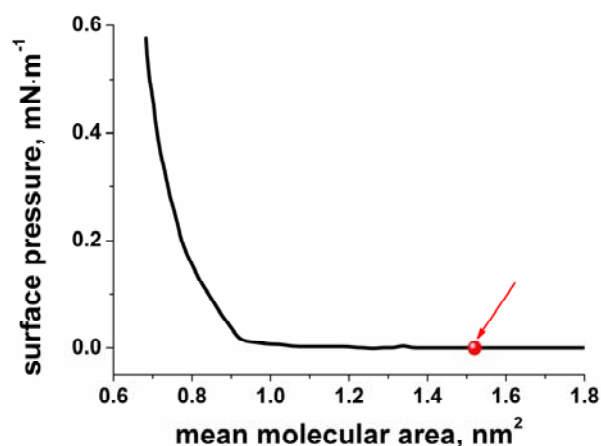


Fig. 3. Compression isotherm of the ZnTPP floating layer. The dot indicates the transfer point

A slight decrease in the area per molecule in the experimentally obtained floating layer, compared to the model one, may be due to 3D-aggregation of ZnTPP. This assumption is confirmed by AFM data of LS-films with one ( $n = 1$ ) and five ( $n = 5$ ) transfers (Fig. 4).

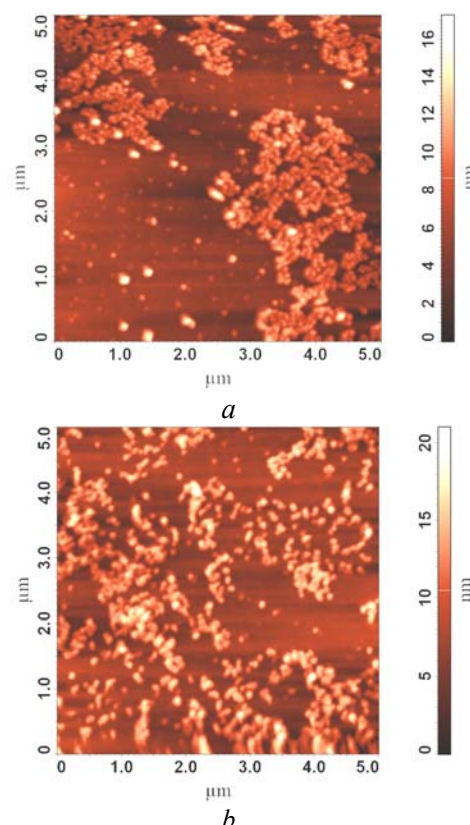


Fig. 4. AFM images of ZnTPP LS-films on a silicon substrate: *a* – one transfer, *b* – five transfers

On the surfaces of all studied LS-films, an imperceptible number of 3D-aggregates with diameter about 1 nm were detected. The distribution of the aggregates on the film surfaces was uneven (Fig. 4). The height of the aggregates increases from 4 nm to 20 nm with the increase of transfers from 1 to 5 as well as the average roughness of the LS-films increases from 1.72 nm (Fig. 5, line 1) to 2.43 nm (Fig. 5, line 2), correspondingly.

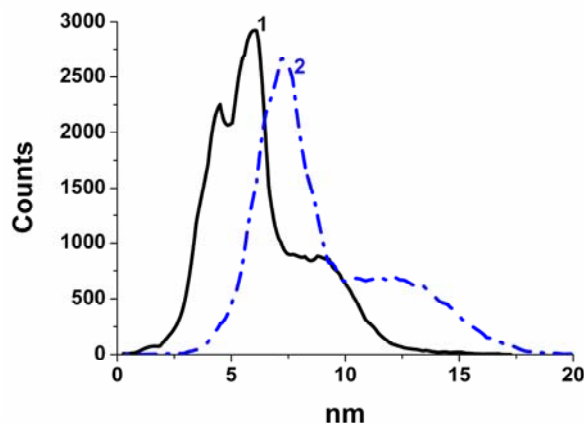


Fig. 5. Roughness distribution for LS-films with one transfer (line 1) and five transfers (line 2)

### *Spectral characteristics of ZnTPP LS-films*

To study the optical properties of ZnTPP LS-films and the aggregation type of ZnTPP molecules, UV-Vis spectra were obtained. The studied films were prepared with different numbers of transfers ( $n = 1-30$ ) of the floating layer. It was shown that the UV-Vis spectra in chloroform solution and in LS-films differ significantly (Fig. 6). The Soret band of LS-films is red shifted by 22 nm in comparison with the solution. This shift indicates the J-type aggregation of ZnTPP molecules in the films.

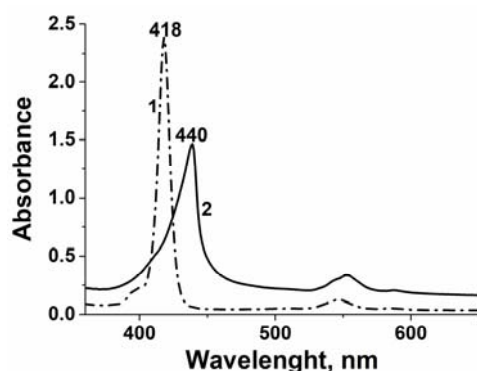


Fig. 6. UV-vis spectra of ZnTPP in chloroform solution (line 1,  $C_{\text{ZnTPP}} = 1.5 \cdot 10^{-5}$  M) and LS-film (line 2,  $n = 30$ )

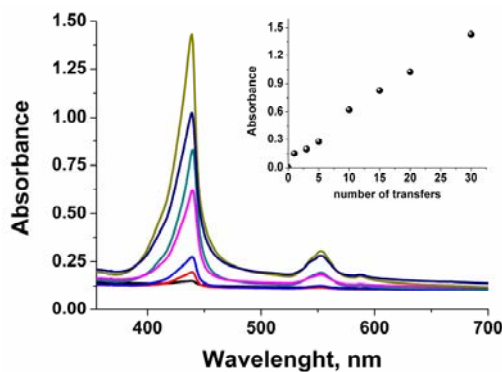


Fig. 7. Change in the UV-Vis spectra of ZnTPP LS-films depending on the number of transfers ( $n = 1-30$ ).  
 Insert – the dependence of optical density (418 nm) on the number of transfers

The optical density of ZnTPP LS-films is influenced by the number of transfers. The linear

dependence (Fig. 7, see the insert) of the optical density indicates that the ZnTPP LS-films are low defective.

### *Sensing properties of ZnTPP in solutions and LS-film*

It is known that porphyrin complexes with transition metals effectively bind nitrogen bases. Monomeric Zn-porphyrins typically bind only one axial ligand to form penta-coordinated complexes [1, 4]. Such ligand can be pyridine or its derivatives.

In this work, the sensing properties of ZnTPP to PyOH were studied by spectrophotometric titration in different media: chloroform and chloroform/water (1:1) (Fig. 8). It was found that the used media do not affect the interaction of ZnTPP with PyOH, but influence the changes in UV-vis spectra and the stability constant of the ZnTPP·PyOH complex. The coordination of ZnTPP with PyOH in both media results in a shift of Soret band by  $\sim 10$  nm in comparison with the ZnTPP chloroform solution. The stability constants of ZnTPP·PyOH complex in chloroform and chloroform/water (1:1) were equal to  $1.4 \cdot 10^4$  and  $2.9 \cdot 10^4 \text{ M}^{-1}$ , respectively.

The axial coordination of a large number of metalloporphyrins, including ZnTPP, has been studied earlier by spectrophotometric method in aromatic solvents (toluene, DMF) [25]. Authors showed that the stability constant of ZnTPP·Py complexes has the highest values in benzene and toluene (5800 and 2525  $\text{l} \cdot \text{mol}^{-1}$ , correspondingly). In this work, we studied the axial coordination of ZnTPP with PyOH in inert media (chloroform and chloroform/water). The obtained stability constant values were 14000 and 29000  $\text{l} \cdot \text{mol}^{-1}$ , respectively.

Therefore, when chloroform is used instead of aromatic solvents, stability constant values increase in several times and binding properties of ZnTPP with PyOH are getting better.

In chloroform solution, ZnTPP molecules are in the monomeric form, but in LS-films they are aggregated. This difference can change the sensing properties of ZnTPP.

The sensing ability of the ZnTPP LS-film ( $n = 15$ ) to PyOH in aqueous solution and to Py vapor was also investigated by spectrophotometric titration.

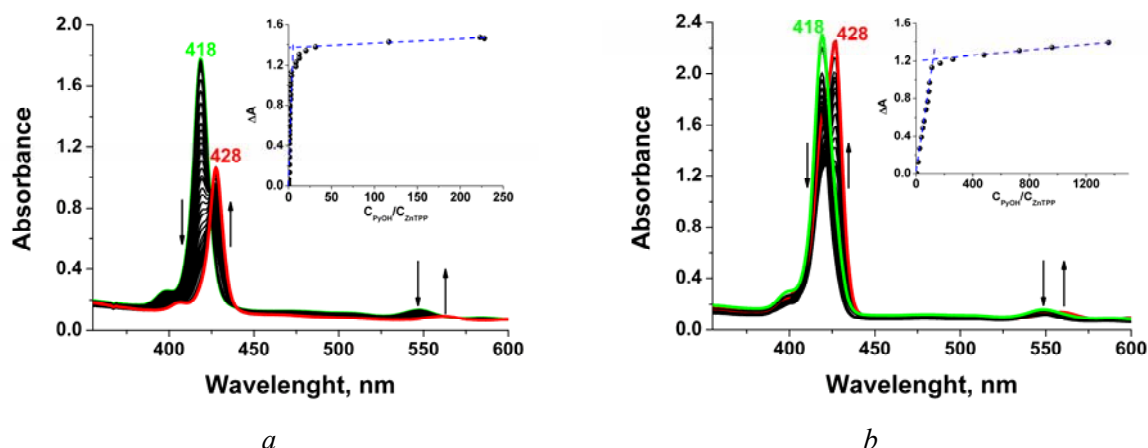


Fig. 8. *a* – Spectral changes in the ZnTPP-PyOH system (chloroform, 298 K) and spectrophotometric titration curve ( $\lambda = 418$  nm,  $C_{\text{ZnTPP}} = 3 \cdot 10^{-6}$  M,  $C_{\text{PyOH}} = 0 \div 1 \cdot 10^{-2}$  M), *b* – spectral changes in the ZnTPP-PyOH system (chloroform/water (1:1), 298 K) and spectrophotometric titration curve ( $\lambda = 418$  nm,  $C_{\text{ZnTPP}} = 3 \cdot 10^{-6}$  M,  $C_{\text{PyOH}} = 0 \div 1 \cdot 10^{-2}$  M)

In the case of PyOH, the ZnTPP LS-film was placed in a quartz cuvette with aqueous solution of PyOH ( $C_{\text{PyOH}}$  from 0 to  $1.5 \cdot 10^{-2}$  M). The cuvette was put into a temperature-controlled spectrophotometer cell and the absorption spectra were registered. The end of sensing process was determined by the absence of changes in the spectra ( $T = 298$  K). Since no changes in the spectra were observed (Fig. 9), it was concluded that the LS-film is not sensitive to PyOH.

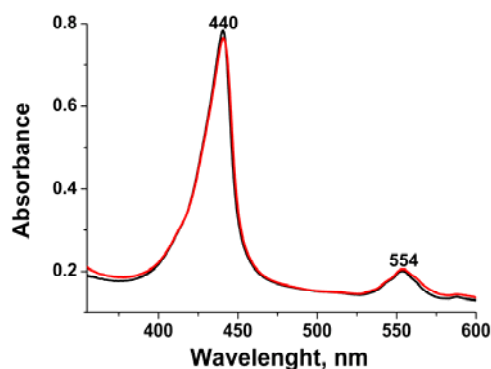


Fig. 9. Spectral changes in the Soret band region during the interaction of the ZnTPP LS-film ( $n = 15$ ) with PyOH in water ( $C_{\text{PyOH}} = 0 \div 1.5 \cdot 10^{-2}$  M)

In the case of Py, the ZnTPP LS-film was treated with pyridine vapors for 1 minute ( $T = 298$  K).

A red shift of the Soret band by 5 nm and the appearance of an additional absorption band in the visible region were observed (Fig. 10). The spectral response evidences the formation of the ZnTPP·Py complex.

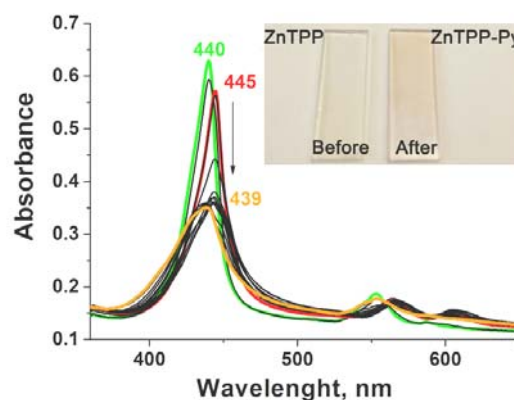


Fig. 10. Spectral changes in the Soret band region during interaction of the ZnTPP LS-film ( $n = 15$ ) with Py vapors

For the first time it was established that the ZnTPP LS-film can be used as a sensor for detecting Py vapors. The obtained data show the potential for applications of ZnTPP films in various scientific and technological fields, including medicine and ecology.

### Conclusions

In this work, the floating layers of Zn(II)-5,10,15,20-tetraphenylporphyrin on the air/water interface were modeled, and the geometric characteristics of their molecular packings were calculated. It was estimated that the area per molecule in the dense *face-on* packing of a monolayer is 1,69 nm<sup>2</sup>, and in the *edge-on* – 0,90 nm<sup>2</sup>. Formation conditions of ZnTPP floating layer at the air/water interface and LS-films on glass and silicon substrates were investigated. Analysis of the compression isotherm of the floating layer showed that ZnTPP molecules are oriented *face-on*. Using UV-Vis spectroscopy, it was established that the LS-films contain J-type aggregates. The surface morphology of the LS-films was studied by AFM. It was found that the average roughness of the LS-films increases by a factor of 1.4, when the number of transfers is increased from one to five. The sensing properties of the LS-film (*n* = 15) to hydroxypyridine and pyridine in aqueous and gas media, respectively, were investigated. It was demonstrated that the LS-film exhibits sensing ability to pyridine vapors. The results obtained can be used in the development of selective sensors for ecological monitoring of environmental pollution.

**Acknowledgments:** This work was supported by the Ministry of Science and Higher Education of the Russian Federation in the framework of the state task of the G. A. Krestov Institute of Solution Chemistry of the Russian Academy of Sciences (No 122040500043-7) and the state task of the Ivanovo State University (No FZZM-2023-0009), RFBR and Ivanovo Region (No 20-47-370002) with the involvement of equipment from the Upper Volga Regional Center for Physical and Chemical Research.

### Список источников / References

1. Maltceva O., Mamardashvili G., Khodov I., Lazovskiy D., Krest'yaninov M., Mamardashvili N., Khodova V., Dehaen W. Molecular recognition of nitrogen – containing bases by Zn[5,15-bis-(2,6-dodecyloxy-phenyl)]porphyrin. *Supramol. Chem.*, 2017, **29**, 360–369. DOI: 10.1080/10610278.2016.1238473.
2. Mamardashvili G.M., Maltceva O.V., Lazovskiy D.A., Khodov I.A., Borovkov V., Mamardashvili N.Z., Koifman O.I. Medium viscosity effect on fluorescent properties of Sn(IV)-tetra(4-sulfonatophenyl)porphyrin complexes in buffer solutions. *J. Mol. Liq.*, 2019, **277**, 1047–1053. DOI: 10.1016/j.molliq.2018.12.118.
3. Mamardashvili G.M., Lazovskiy D.A., Maltceva O.V., Mamardashvili N.Zh., Koifman O.I. The Sn(IV)-tetra(4-sulfonatophenyl) porphyrin complexes with antioxidants: Synthesis, structure, properties. *Inorg. Chim. Acta*, 2019, **486**, 468–475. DOI: 10.1016/j.ica.2018.11.003.
4. Mamardashvili G.M., Maltceva O.V., Mamardashvili N.Z., Nguyen N.T., Dehaen W. Cation assisted complexation of octacarbazolyphenyl substituted Zn(II)-tetraphenylporphyrin with [2,2,2]cryptand. *RSC Adv.*, 2015, **5**, 44557–44562. DOI: 10.1039/C5RA05687J.
5. Sengupta S., Würthner F. Chlorophyll J-aggregates: From bioinspired dye stacks to nanotubes, liquid crystals and biosupramolecular electronics. *Acc. Chem. Res.* 2013, **46**, 2498–2512. DOI: 10.1021/ar400017u.
6. Tian J., Zhang W. Synthesis, self-assembly and applications of functional polymers based on porphyrins. *Prog. Polym. Sci.*, 2019, **95**, 65–117. DOI: 10.1016/j.progpolymsci.2019.05.002.
7. Tsivadze A.Yu. Supramolecular metal complex systems based on crown-substituted tetrapyrroles. *Russ. Chem. Rev.*, 2004, **73**, 6–25. DOI: 10.1070/RC2004v073n01ABEH000862.
8. Kobayashi N. Dimers, trimers and oligomers of phthalocyanines and related compounds. *Coord. Chem. Rev.*, 2002, **227**, 129–152. DOI: 10.1016/S0010-8545(02)00010-3.
9. Imamura T., Fukushima K. Self-assembly of metallopyridylporphyrin oligomers. *Coord. Chem. Rev.*, 2000, **198**, 133–156. DOI: 10.1016/S0010-8545(99)00211-8.
10. Meng T., Leiab P., Zeng Q. Progress in the self-assembly of porphyrin derivatives on surfaces: STM reveals. *New J. Chem.*, 2021, **45**, 15739–15747. DOI: 10.1039/D1NJ03111B.
11. Mamardasvili G.M., Mamardashvili N.Z., Koifman O.I. Macrocyclic receptors for identification and selective binding of substrates of different nature. *Molecules*, 2021, **26**, 5292. DOI: 10.3390/molecules26175292.
12. Cai J., Chen H., Huang J., Wang J., Tian D., Dong H., Jiang L. Controlled self-assembly and photovoltaic characteristics of porphyrin derivatives on a silicon surface at solid–liquid interfaces. *Soft Matter*, 2014, **10**, 2612–2618. DOI: 10.1039/C3SM53061B.
13. Wei W., Sun J., Fan H. Cooperative self-assembly of porphyrins and derivatives. *MRS Bulletin*, 2019, **44** (3), 178–182. DOI: 10.1557/mrs.2019.39.
14. Jiang Y.-B., Sun Z. Self-assembled porphyrin and macrocycle derivatives: From synthesis to function. *MRS Bulletin*, 2019, **44** (3), 167–171. DOI: 10.1557/mrs.2019.44.
15. Kundu S. Semi-reversible collapse of preformed cobalt stearate Langmuir monolayer on water surface. *J. Mol. Struct.*, 2021, **1238**, 130414.



- DOI: 10.1016/j.molstruc.2021.130414.
16. Shokurov A.V., Kutsybala D.S., Martynov A.G., Bakirov A.V., Shcherbina M.A., Chvalun S.N., Gorbunova Y.G., Tsivadze A.Yu., Zaytseva A.V., Novikov D., Arslanov V.V., Selektor S.L. Long-sought redox isomerization of the europium(III/II) complex achieved by molecular reorientation at the interface. *Langmuir*, 2020, **36**, 1423–1429.  
DOI: 10.1021/acs.langmuir.9b03403.
17. Ma K., Wang R., Rao Y., Zhao W., Liu S., Jiao T. Langmuir-Blodgett films of two chiral perylene bisimide-based molecules: Aggregation and supramolecular chirality. *Colloids and Surfaces A: Physicochem. Eng. Asp.*, 2020, 591, 124563.  
DOI: 10.1016/j.colsurfa.2020.124563.
18. Giancane G., Valli L. State of art in porphyrin Langmuir-Blodgett films as chemical sensors. *Adv. Colloid Interface Sci.*, 2012, **171–172**, 17–35.  
DOI: 10.1016/j.cis.2012.01.001.
19. Giancane G., Borovkov V., Inoue Y., Valli L. Conformational switching in bis(zinc porphyrin) Langmuir-Schaefer film as an effective tool for selectively sensing aromatic amines. *Colloid Interface Sci.*, 2012, **385**, 282–284.  
DOI: 10.1016/j.jcis.2012.06.081.
20. Ghosh A., Mahato P., Choudhury S., Das A. Comparative study of porphyrin derivatives in monolayers at the air–water interface and in Langmuir-Blodgett films. *Thin Solid Films*, 2011, **519** (22), 8066–8073. DOI: 10.1016/j.tsf.2011.02.082.
21. Capan İ., Tarımcı Ç., Capan R. Fabrication of Langmuir-Blodgett thin films of porphyrins and investigation on their gas sensing properties. *Sensors and Actuators B: Chemical*, 2010, **144** (1), 126–130.  
DOI: 10.1016/j.snb.2009.10.046.
22. Maiorova L., Kobayashi N., Zyablov S., Bykov V., Nesterov S., Kozlov A., Devillers Ch., Zavyalov A., Alexandriysky V., Orena M., Koifman O. Magnesium porphine supermolecules and two-dimensional nanoaggregates formed using the Langmuir-Schaefer technique. *Langmuir*, 2018, **34** (31), 9322–9329.  
DOI: 10.1021/acs.langmuir.8b00905.
23. Shokurov A.V., Kutsybala D.S., Kroitor A.P., Dmitrienko A.A., Martynov A.G., Enakieva Y.Y., Tsivadze A.Y., Selektor S.L., Gorbunova Y.G. Spin crossover in nickel(II) tetraphenylporphyrinate via forced axial coordination at the air/water interface. *Molecules*, 2021, **26** (14), 4155 (13 p.).  
DOI: 10.3390/molecules26144155.
24. Kazak A.V., Marchenkova M.A., Smirnova A.I., Seregin A.Yu., Rogachev A.V., Klechkovskaya V.V., Arkharova N.A., Warias J.E., Murphy B.M., Tereschenko E.Yu., Usol'tseva N.V., Kovalchuk M.V. Floating layers and thin films of mesogenic mix-substituted phthalocyanine holmium complex. *Thin Solid Films*, 2020, **704**, 137952 (8 p.).
25. Mamardashvili G.M., Mamardashvili N.Zh., Koifman O.I. Supramolecular porphyrin complexes. *Russ. Chem. Rev.*, 2005, **74** (8), 765–780.  
DOI: 10.1070/RC2005v074n08ABEH001056.

**Contribution of the authors:**

<sup>1</sup>Maltceva O. V. – conducting research, preparing illustrations, editing the text of the article.

<sup>2</sup>Nikitin K. S. – conducting research, preparing illustrations, editing the text of the article.

<sup>3</sup>Kazak A. V. – editing the text of the article

<sup>4</sup>Mamardashvili N. Zh. – development of the concept of scientific work, funding acquisition, writing, reviewing and editing the text of the article.

<sup>5</sup>Usol'tseva N. V. – funding acquisition, writing and editing the text of the article.

**The authors declare no conflicts of interests.**

<sup>1</sup><https://orcid.org/0000-0002-4983-8969>

<sup>2</sup><https://orcid.org/0000-0002-0980-3366>

<sup>3</sup><https://orcid.org/0000-0002-3504-7998>

<sup>4</sup><https://orcid.org/0000-0001-9778-5227>

<sup>5</sup><https://orcid.org/0000-0001-8963-8024>

Поступила 17.04.2023; одобрена 17.05.2023; принята 22.05.2023.  
Received 17.04.2023; approved 17.05.2023; accepted 22.05.2023.